HYDROLOGICAL PROCESSES
Hydrol. Process. **28**, 5972–5984 (2014)
Published online 15 November 2013 in Wiley Online Library
(wileyonlinelibrary.com) DOI: 10.1002/hyp.10090

Temporal variation of suspended sediment transport in the Koga catchment, North Western Ethiopia and environmental implications

Eleni Yeshaneh,[1]* Alexander Eder[1,2] and Günter Blöschl[1]

[1] *Vienna University of Technology, Centre for Water Resources Systems, Karlsplatz 13, 1040 Vienna, Austria*
[2] *Institute for Land and Water Management Research, Pollnberstrasse 1, 3252 Petzenkirchen, Austria*

Abstract:

Event sediment transport and yield were studied for 45 events in the upstream part of the 260 km^2 agricultural Koga catchment that drains to an irrigation reservoir. Discharge and turbidity data were collected over a period of more than a year, accompanied by grab sampling. Turbidity was very well correlated with the sediment concentrations from the samples ($r = 0.99$), which allowed us to estimate the temporal patterns of sediment concentrations within events. The hysteresis patterns between discharge and sediment concentrations were analysed to provide insight into the different sediment sources. Anticlockwise patterns are the dominant hysteresis patterns in the area, suggesting smaller contributions of suspended sediment from the river channels than from the hillslopes and agricultural areas. Complicated types of hysteresis patterns were mostly observed for long events with multiple peaks. For a given discharge, sediment yields in August and September, when the catchment was almost completely covered with vegetation, were much smaller than during the rest of the rainy season. The hysteresis patterns and timing suggest that the sediment availability from the agricultural areas and hillslopes affects sediment yields more strongly than does peak discharge. Two distinct types of sediment rating curves were observed for the season when the agricultural land was covered with vegetation and when it was not, indicating the dominating contribution of land use/cover to sediment yields in the catchment. The rate of suspended sediment transport in the area was estimated as 25.6 t $year^{-1}$ ha^{-1}. Copyright © 2013 John Wiley & Sons, Ltd.

KEY WORDS event suspended sediment transport; sediment yield; hysteresis pattern

Received 6 June 2013; Accepted 9 October 2013

INTRODUCTION

Many countries suffer from land degradation and from associated processes such as gullying, flooding and sedimentation (Sadeghi *et al*., 2008). The economic implication of this is more serious in developing countries because of a lack of capacity to cope with it and also to replace lost nutrients (Tamene and Vlek, 2008). Soil erosion in the Ethiopian highlands is a natural phenomenon due to erosive rainfall and steep and undulating topography but is enhanced under agricultural systems that reduce protective soil cover (Guzman *et al*., 2013). The intensified use of the already stressed resources due to high population growth in Ethiopia makes soil erosion the most serious environmental problem affecting the quality of soil, land and water resources upon which humans depend for their subsistence (Shiferaw and Holden, 1999; Tamene and Vlek, 2008). The annual rate of soil loss is significantly higher than the annual rate of soil formation rate in the country.

Estimates of sediment yield and its temporal variation are needed for various purposes including design of erosion control structures (Russel *et al*., 2001), river morphological computations and evaluation studies of the effects of various land use management practices (Gao and Pasternack, 2007; Sadeghi *et al*., 2008; Gao and Puckett, 2011). Understanding and quantifying erosion is important in highly erodible catchments that eventually contribute to siltation of downstream reservoirs (Lopez-Tarazon *et al*., 2009; Gao and Puckett, 2011; Guzman *et al*., 2013), especially with storms of high rainfall intensity where run-off occurs over highly unconsolidated sediments on agricultural areas (Nyssen *et al*., 2007). Once sediments reach the reservoirs, siltation becomes a long-term socio-economical problem because it reduces water storage capacity (Lopez-Tarazon *et al*., 2009).

Sediment supply in a catchment is heterogeneous in time and space depending on climate, land use and a number of landscape characteristics such as slope, topography, soil type, vegetation and drainage conditions

* Correspondence to: Eleni Yeshaneh, Vienna University of Technology, Centre for Water Resources Systems, Karlsplatz 13, 1040 Vienna, Austria.
E-mail: elleniyeshaneh@yahoo.com

(Marttila and Klove, 2010). The investigation of suspended sediment concentration (SSC) discharge relationships of individual events allows inference of the dominant origins and processes contributing to suspended sediment (SS) dynamics of a basin (Lefrancois *et al*., 2007; Sadeghi *et al*., 2008; Smith and Dragovich, 2009; Gao and Puckett, 2011). The relationship between discharge and sediment concentration usually presents a hysteretic loop, which can be classified according to their symmetry, and their clockwise or anticlockwise hysteresis (Jansson, 2002; Lefrancois *et al*., 2007; Smith and Dragovich, 2009; Gentile *et al*., 2010). Variability in the SSC-discharge relationship has been studied to identify sediment origins on catchments of varying sizes. The features of the hysteresis loops have been attributed to the location of the sediment source in the basin, the river bed or the river banks (Jansson, 2002; Smith and Dragovich, 2009; Gao and Puckett, 2011). Clockwise loops have often been related to the depletion of available sediments in the catchment or in the stream channel or the successive reduction of the erosive effect of rainfall (Jansson, 2002; Gao and Josefson, 2012). An anticlockwise hysteresis usually reflects sufficient hillslope sediment supply, delayed in-channel sediment resuspension caused by the late break-up of biofilms, additional sediment sources from channel banks or tributaries or variable rainfall patterns (Gao and Josefson, 2012). The clockwise hysteresis between SSC and discharge is regarded as a normal condition for most fluvial systems where SS transport is mainly caused by precipitation-induced flooding (Gao and Puckett, 2011).

In the Ethiopian highlands, sediment delivery depends on discharge, the onset of rainfall, land use and land cover, which vary between rainfall seasons (Awulachew *et al*., 2010). Because of this, sediment rating curves are complex, and sediment budgets have rarely been established (Nyssen *et al*., 2007). Although a number of studies have been performed in small catchments (Gao and Pasternack, 2007; Lefrancois *et al*., 2007; Sadeghi *et al*., 2008; Smith and Dragovich, 2009; Eder *et al*., 2010; Marttila and Klove, 2010), much less is known about the sediment dynamics in medium scale catchment (Gao and Josefson, 2012). The aim of this paper is to quantify the temporal variability of sediment yield from a medium-sized catchment in the Ethiopian highlands and identify the dominant (possible) sediment sources and generation mechanisms. This paper also assesses the future environmental implications of sediment delivery in the study area.

MATERIALS AND METHODS

The study area

Location, climate and topography. The considered study area is 9838 ha in size and represents the upstream part of the 260-km^2 Koga catchment (Figure 1) in northwestern Ethiopia. The Koga catchment is a typical catchment for the Ethiopian Highlands, 72% of which is used for subsistence agriculture. The Koga River is a tributary of the Gilgel Abbay, which flows northwest into Lake Tana and lies in the upper part of the Blue Nile (Abbay) watershed.

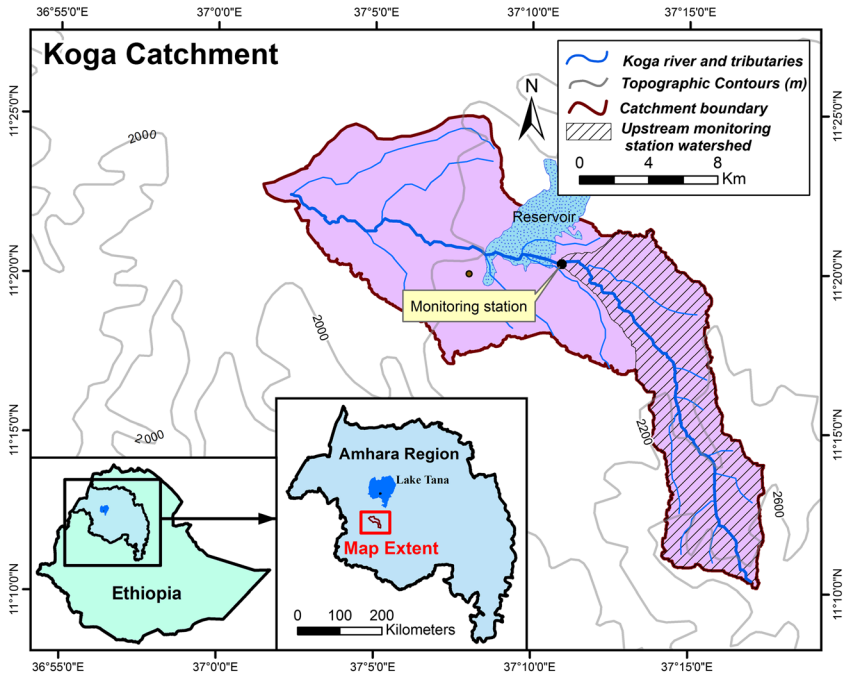

Figure 1. Location map of the Koga catchment

The climate of the Koga catchment falls within the Woina Dega [cool semi-humid, 1500 to 2400 m above sea level (a.s.l.)] and Dega zones (cool, above 2400 m a.s.l.). The majority of the catchment area lies within the Woina Dega zone and is characterized by distinct dry and wet seasons. The dry seasons occur between November and April and the wet season between May and October; small rains occur sporadically during April and May. The mean annual rainfall for the catchment is 1550 mm (period 2006–2010). The mean daily temperature is 18.25 °C. The monthly mean maximum temperature varies from 30.0 °C in March to 23.7 °C in August. The monthly mean minimum temperature varies from 5.4 °C in December to 13.1 °C in May and June.

Although the land elevation of the Koga catchment varies from 1875 m a.s.l. at the mouth of the Koga River to 3215 m a.s.l. at its highest point on the watershed divide, the considered study area has its lowest elevation of 2015 m a.s.l. at its mouth where it joins the Koga reservoir. The Koga reservoir (Figure 1) is used for irrigation of the downstream areas. The Koga River flows at a distance of 26 km before it joins the Koga irrigation reservoir and a distance of 49 km before it joins the Gilgel Abbay, which eventually flows into Lake Tana. The Koga catchment is generally elongated with a pronounced narrowing above the Village of Rim where the mean width of the catchment is only 3.8 km. The course of the Koga River is northerly up to the village of Rim and then westerly to Wetet Abbay.

Geology and soils. The regional geology of the Koga catchment comprises extensive flow type, volcanic (extrusive) rocks mainly of the Ashangi Group; these were deposited during the palaeocene-Oligocene-Miocene (teritiary) stages of geological time. The Ashangi group comprises the older volcanic rocks, which were formed by lava and debris, ejected from fissural volcanic eruptions. The choke shield volcanic group, deposited during the Miocene and Pliocene, has covered a small area of the upper Koga catchment in the eastern part. The shield volcanic group consists mainly of pyroclastic basalt and is petrographically similar to the Ashangi group. The soil types within the upper part of the Koga catchment we studied are Luvic Phaeozems (Typic Argiustolls), Chromic Cambisols (Fluventic and Typic Ustropepts), Lithic Leptosols (Lithic Ustropepts), Haplic Alisols (Typic Paleustults), Eutric Vertisols (Ustic Tropaquepts) and Eutric Gleysols (Typic Tropaquepts). These soils have clay to clay loam texture with the exception of Eutric Gleysols (Typic Tropaquepts) that has clay to sandy clay loam texture.

Population and tillage practices. The total population of the Mecha woreda, within which the Koga catchment is located, is 292 000, of which 269 404 live in the rural part, whereas 22 677 live in the urban part (CSA, 2007). Subsistence rain fed production of cereals comprising teff, maize, barley and millet, as well as pulses, oilseeds and some legumes is dominant in the area, whereas irrigated agriculture takes up a small percentage of the cultivated area of the Koga catchment. Soil tillage is performed with oxen-drawn ploughs. There exist some attempts to prevent soil erosion through soil and water conservation structures such as stone stacks along with tree planting (Figure 11e), storm water diversion channels, soil bunds (Figure 11c), channel and orchard terraces and contour cultivation, though not based on sufficient study as to which of these are most effective in controlling soil erosion in the catchment. Crop cultivation is the main source of income followed by livestock for the poor farmers in the area.

Methods

Event data collection and developing a relationship between turbidity measurements and SSC. A hydrological monitoring station consisting of pressure transducer, DTS-turbidity sensor (Digital Turbidity Sensor), axiom data logger and staff gauge has been installed along a relatively stable and steep cross section in the Koga catchment (Figure 1). The station was installed just above the Koga reservoir along the river that serves for irrigation of the downstream areas. The DTS-turbidity sensor was put around the middle of the horizontal cross section and was moved up or down in the different seasons depending on the flow conditions so that it remained, approximately, at the midpoint of the vertical section of the flow. Although it is expected that there is a difference in SSCs both vertically and horizontally along river cross sections, some researchers have indicated that the difference in SSC may be small at low flows (Gao and Josefson, 2012), with an average spatial variation of 9% of the mean of all samples collected along the vertical and horizontal cross sections at a time (Lopez-Tarazon *et al*., 2009). Gao *et al*. (2007) indicated that grab samples at a point of a cross section can be regarded as the averaged sample over the cross section at any time. For high flow conditions, mixing increases, which will make the measurements from the turbidity sensors more representative of the whole cross section, although entrainment from the river bed and river bank may lead to layering of the sediment concentrations. Given that most of the sediment comes from the hillslopes (see later in the paper), the latter effect is probably small. Some biases due to the sensor position may still have occurred, which would be of interest to analyse in more detail. The DTS-turbidity sensor was factory calibrated, and it was able to prevent biofilm growth on the sensor by a wiper that wipes the sensor system every 30 s. A rating curve was developed for the cross section using Manning's equation accompanied by several velocity measurements for various water levels (high and low flows) using current metre and

floating devices. We set up the monitoring station in a relatively stable and steep cross section to minimize sediment deposition along the cross section. Considering the possibility of inundations at the monitoring station, the data logger was placed at considerable height. Although there were several events that produced nearly bank full peak flows, none of the events exceeded the bank full discharge at the monitoring station in the study period. This was because of upstream inundations resulting from small weirs across the stream that have been used for irrigation during the dry season by individual upstream farmers. The shapes of the hydrographs suggest, however, that the upstream flows into the flood plains were relatively small. The bank full discharge is 47.6 $m^3 s^{-1}$ at the monitoring station.

Using the Axiom data logger, we were able to have a continuous record of water turbidity expressed in nephelometric turbidity units and water level data in metres for 1 year starting from October 2011–2012. In addition, 257 water grab samples were collected manually with 500 ml plastic bottles from along the mid of the river for 25 events. Four to 12 samples per event were collected at 10- to 15-min intervals. Sample collection was based on convenience for collection either for the rising limb, falling limb or both without preference to any of the rainfall events. The sampling process did not cover the whole duration of an event and was much less than the total duration of any of the 45 events as also seen on Figures 2(a) and (c), 3(a) and 4. Samples were collected either for the rising limbs, peaks, for

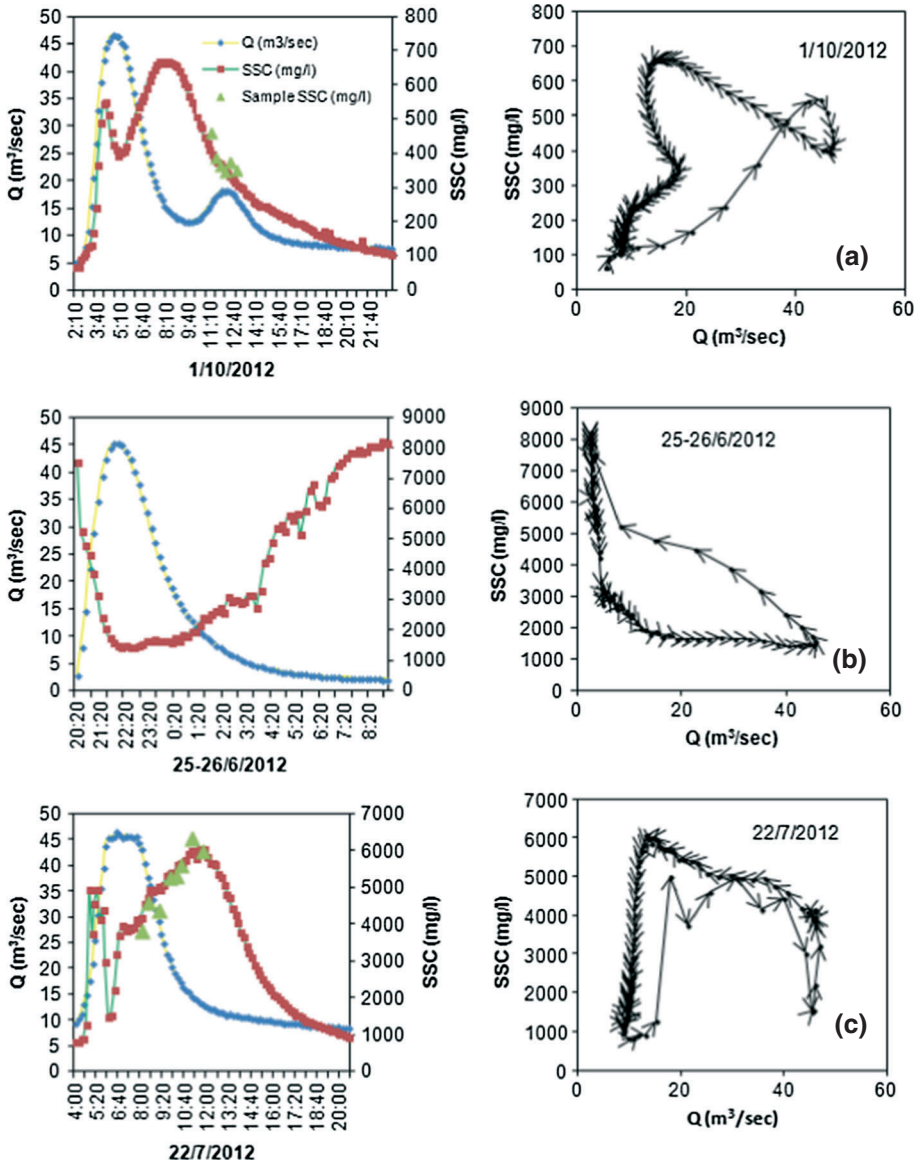

Figure 2. Suspended sediment concentration (SSC) – discharge hysteresis loops of (a) anticlockwise-clockwise-anticlockwise and (b) and (c) anticlockwise patterns of some of the events

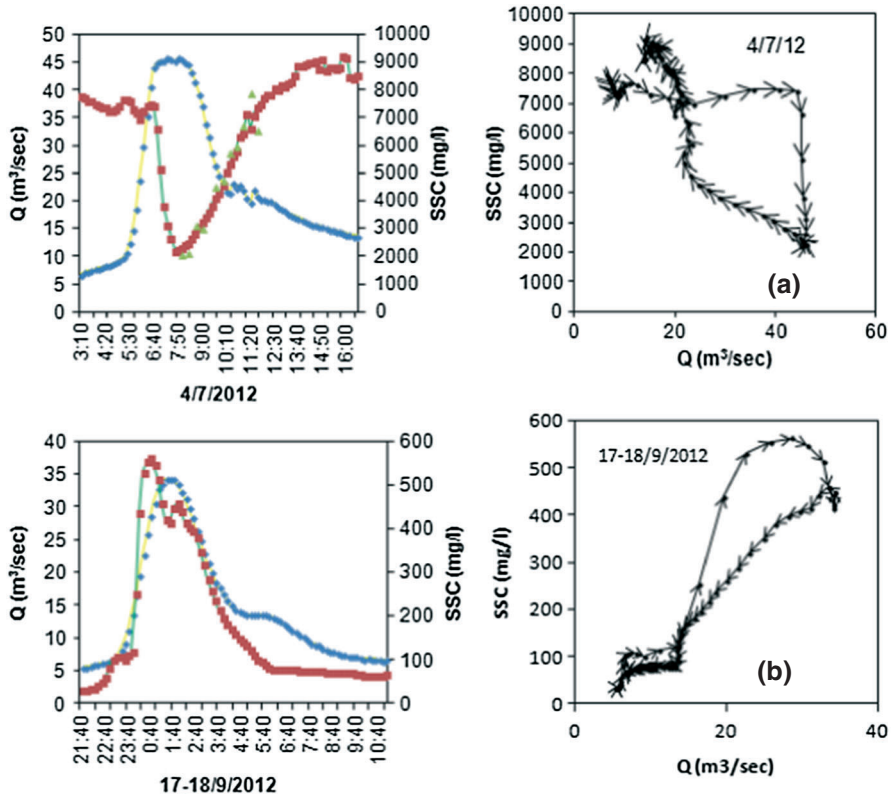

Figure 3. Suspended sediment concentration (SSC) – discharge hysteresis loops of (a) clockwise-anticlockwise-clockwise and (b) clockwise patterns

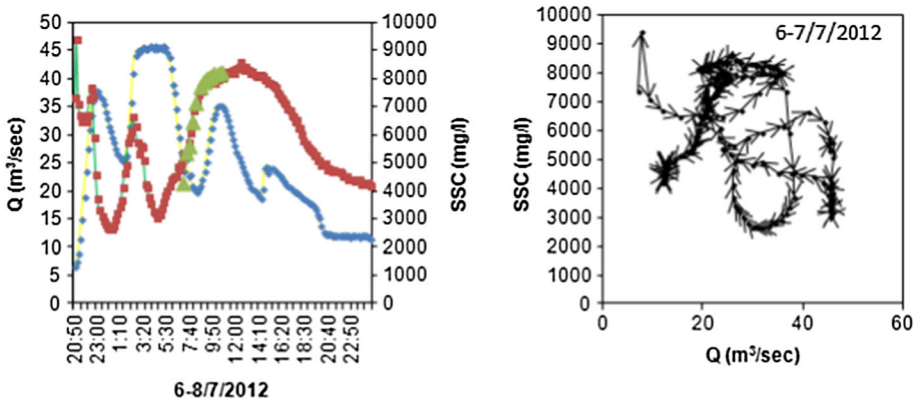

Figure 4. Suspended sediment concentration (SSC) – discharge hysteresis loop of a complicated pattern

the falling limbs or combinations of these three for the different events that in turn makes the sampling process representative of the 45 events for creating SSC-turbidity relationship. From the 257 samples collected, 222 were analysed for SSC at the national and regional water bureaus. The remaining 35 samples were disregarded because leakage of part of the sample occurred before reaching the labs due to a failure to close the bottles tightly.

A relationship between turbidity measurements and SSC was developed on the basis of the SSC values of the collected samples. Out of the 222 samples analysed for SSC, 179 samples were used for establishing the relationship between turbidity and SSC. The remaining 43 samples were excluded as they were either outliers or had extremely low turbidity readings for events with extremely large SSC values (up to 22 000 mg l^{-1}). Using the 179 samples, we were able to get a very good (Figure 5) correlation coefficient ($R^2 = 0.987$) between turbidity values and sample SSC values. Because of the excellent correlations, estimated sediment concentrations for events without samples were also considered reliable. Although texture analysis was not carried out on the SS from the

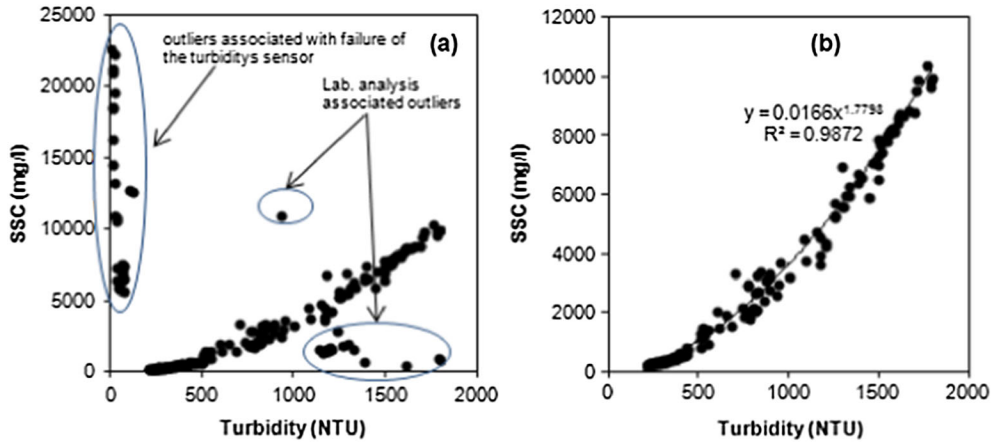

Figure 5. Suspended sediment concentration – turbidity relationship before (a) and after (b) removing outliers

water grab samples, previous soil studies in the catchment suggest that 85% of the upper catchment has a soil texture ranging from clay to clay loam (Acers International Limited & Shawel Consult, 1995). Soil texture analysis made on 12 soil samples we took from the different soil types in the catchment indicated that the upper catchment does have soil texture ranging from heavy clay to loam. This reduces the potential effect coarser SSs would have had on the turbidity-SSC relationship especially during high flows. Turbidity values of some of the events in June exceeded the measurement range of the turbidity sensor, and in that case, the turbidity sensor recorded only its maximum limit (1797 nephelometric turbidity units). For those events, the suspended sediment yield (SSY) is a little underestimated.

SSC-discharge hysteresis analysis. Hysteresis patterns of SSC were generated and analysed for a link to the likely sediment sources and transport processes. Hysteresis analysis was performed by the classic visual analysis as it was found to give more reliable information than other methods (Gao and Josefson, 2012).

Calculating SSY and examination of the relationship between SSY and Q_{peak}. We summed up the SSY calculated every 10 min throughout the event to generate the SSY of each event. To have a good estimate of total sediment yield of each event, we examined whether or not there is a trend in SSC beginning from an hour before the start of the event until the start of the event. If there was a decreasing trend in sediment concentration before the start of the event, the corresponding sediment yields were calculated from the sediment concentrations, and the rate of decrease in the sediment yield was considered when subtracting the amount of sediment before the start of the event from the sediment yield of the event. If there was no trend in the sediment yield before the start of the event, the amount of sediment yield just before the start of the event was subtracted from the event flow. This is believed to increase the accuracy of the estimated event sediment yield. The relationship between SSY and Q_{peak} was then analysed for each event and for each month to identify the seasonal variation and sediment sources in the study area. In this study, we considered only SS load that makes the major part of the total sediment load. However, it should be noted that transport of materials such as soil aggregates and sand and gravel size materials as a bed load may contribute to the total sediment load. We calculated the SSY for each event to determine the major sediment sources because sediment transport in the study area is mainly associated with a few erosive events throughout the hydrological year. The yearly sediment yield was calculated on the basis of the continuous discharge and turbidity values for one hydrological year using the established relationship with sample SSC. For the few missing SSC data for the June events when the turbidity sensor failed, we used the rating curve we developed on the basis of Q_{peak} for calculating the sediment yield for that particular time. This might add some uncertainty to the SSY estimates for these points in time.

The main rainy season in the catchment is June, July and August. The rainfall starts to decrease in September and significantly decreases in October, with little or no rainfall in November. We started data collection in October 2011 when the rainfall was decreasing. The major rainy season started in June 2012, which was a little later than usual. This was the time when the crop fields were ploughed in preparation for cultivation in the major rainy season. The cultivated land and most of the pasture was completely devoid of vegetation in early June. Although the pasture land is green by mid-June, crops start to grow towards the end of June, and most of the cultivated crop fields are at an early stage of crop growth and do not turn green until mid-July. From around mid-July, the cultivated land begins to be covered with vegetation. Around mid-August until the

end of September, the catchment is almost completely green and covered with vegetation. Crop harvest of most of the crops begins in early October. Part of the cultivated land that is close to the river became swampy from mid-July until the end of September and was ploughed and made ready for sowing in early October. These vegetation dynamics were accounted for when interpreting SSY.

RESULTS AND DISCUSSIONS

SSC-discharge hysteresis analysis

We observed five types of hysteresis: anticlockwise (A), clockwise (C), two types of eight-shaped anticlockwise-clockwise-anticlockwise (ACA) and clockwise-anticlockwise-clockwise (CAC) and complicated patterns. Whereas most of the events with single peak discharge and short peak discharge time showed any of the first four hysteresis patterns, events with multiple peak discharges or prolonged single discharge time showed complicated patterns.

Although the September events showed all the above-named five types of hysteresis (Table I and Figure 6(a)), the events with clockwise hysteresis showed much larger sediment yields than those with anticlockwise hysteresis and other types of hysteresis for similar peak discharges (Table I). Flow for the event 27–28/9/2012 with a peak flow of $16\,m^3\,s^{-1}$ and clockwise hysteresis had a sediment yield of 89.8 t, whereas the event 10/9/2012 with the same peak flow and with anticlockwise hysteresis had a sediment yield of only 17.6 t. The same is true of the event 4–5/9/2012 with a peak flow of $30.27\,m^3\,s^{-1}$ and a clockwise hysteresis (flow duration of 8:50 h) as compared with the event of 1/9/2012 that had the same peak flow but anticlockwise hysteresis (flow duration of 12:20 h). This suggests more sediment is generated from the river channels than from other sources in September. This is because crop vegetation cover in September is higher than in the other months of the year, and sediment contribution from the agricultural areas is less in this month than in the previous months.

Sediment yields after mid-August are much smaller than sediment yields before mid-August for similar peak flows (Table I). Nearly all the August events showed complicated hysteresis patterns except two of them in late August that showed anticlockwise patterns (Figure 6(a)). Anticlockwise hysteresis patterns showed much less sediment yield than those with complicated patterns.

July events mainly showed anticlockwise and complicated patterns but for events with similar peak flows, the ones with complicated hysteresis types showed higher amounts of sediment yield, followed by events with anticlockwise hysteresis patterns. Events with clockwise hysteresis had the lowest amount of sediment yield, indicating channel sources are less important sources than other sources for this month, while at the same time it indicates that complicated environmental conditions are involved in sediment transport. All the four June events showed three types of hysteresis patterns (anticlockwise, clockwise and complicated). A large event in June with a complicated hysteresis pattern showed much greater sediment yield than an event with similar magnitude but an anticlockwise pattern. The clockwise hysteresis patterns of June and July events tend to be associated with sediment entrainment from deposition of antecedent run-off events, especially when there is a relatively short time gap between successive events that reduces the time of subsurface flows to transport the deposited sediments before the succeeding events. For example, the Q_{peak} time gap between the successive events 27/6/2012 to 27–28/6/2012 and the successive events 1–2/7/2012 to 2–3/7/2012 is 23 and 21 h, respectively, and they resulted in clockwise patterns to follow anticlockwise patterns in the first events. However, this pattern does not seem to be consistent for the consecutive events of 25–26/6/2012 to 27/6/2012 with a Q_{peak} time gap of 30 h, which both showed anticlockwise hysteresis patterns. More work would be needed to shed light on the effect of consecutive events on hysteresis patterns. Regardless of peak flow or duration of flows, all October events and the one November event showed ACA hysteresis pattern, except for the small mid-October event that showed an anticlockwise hysteresis.

In general, anticlockwise hysteresis, including more of anticlockwise type ACA patterns, dominates in the study area, implying channel sources are less important than other sources. We also observe from Figure 6(b) that the percentage of complicated hysteresis patterns is high for events with relatively high peak flows indicating complicated processes involved in sediment transport with increased amount of peak flows.

SSY and relationship with Q_{peak}

The relationship between SS and discharge reflects the overall pattern of erosion and SS delivery operating in the catchment area, shedding light on basin SS response (Walling and Webb, 1982). In our study area, there was a good relationship between the peak flows and sediment concentration for the 15 events in September with a correlation coefficient of 0.88. All the September events, whether high or low, were associated with lower sediment yields than similar events in other months of the rainy season. The hysteresis patterns suggest that the contribution of sediment yield from the river channel is more important than contributions from the agricultural areas and hillslopes for this month. The dominance of channel erosion as a sediment source may explain the good correlation between sediment yield and peak flow in September.

Table I. Characteristics of discharge and sediment concentration and hysteresis patterns of the 45 events in the Koga catchment

Date	Q_{mean} ($m^3 s^{-1}$)	Q_{peak} ($m^3 s^{-1}$)	SSC mean ($mg l^{-1}$)	SSY (tonnes)	Hysteresis pattern	Duration (h)
8/10/2011	10.8	15.2	3987	3647	A-C-A	20:20
8–9/10/2011	10.0	16.1	1405	820	A	15:50
1/10/2012	16.23	46.8	322	446	A-C-A	20:40
2/10/2012	13.0	28.3	252	239	A-C-A	19:40
15/10/2011	0.3	0.7	636	7	A	8:20
30–31/10/2011	5.8	17.9	8175	1924	C	10:30
3/11/2011	1.4	3.7	4416	388	A-C-A	16:20
25–26/6/2012	13.8	45.5	4228	1502	A	12:40
27/6/2012	3.7	6.2	4602	468	A	9:10
27–28/6/2012	5.1	13.0	3024	479	C	16:00
30/6/2012	19.6	45.9	3866	3080	Complicated	15:50
1–2/7/2012	10.2	23.7	2785	831	A	8:50
2–3/7/2012	14.1	25.8	3581	1032	C	6:00
3/7/2012	22.0	32.6	7104	8778	C-A-C	15:30
4/7/2012	22.8	45.9	6814	3831	C	13:20
6/7/2012	12.2	22.5	8719	1445	A	9:30
6–7/7/2012	25.8	38.0	5918	9630	Complicated	28:00
8/7/2012	19.5	43.6	5635	5352	A	18:40
14–15/7/2012	32.4	46.5	6420	12146	Complicated	20:30
15–16/7/2012	30.49	45.6	3704	7675	Complicated	24:00
22/7/2012	19.16	46.7	3437	3804	A	16:30
25–26/7/2012	30.02	46.4	1930	6717	Complicated	30:00
6/8/2012	17.52	44.9	792	1231	Complicated	18:40
17–18/8/2012	34.09	44.0	599	848	Complicated	12:40
23–24/8/2012	22	46.7	330	1087	Complicated	30:20
26/8/2012	21.2	46.6	469	511	A	12:40
28/8/2012	22.9	46.0	479	675	Complicated	14:50
31/8/2012	13.5	20.3	214	70	A	7:30
31/8/2012–1/9/2012	25.0	46.7	454	697	Complicated	17:40
1/9/2012	15.5	31.1	258	136	A	12:20
2–3/9/2012	27.4	47.0	452	536	A-C-A	12:00
3–4/9/2012	9.8	10.4	128	28	Complicated	11:40
4–5/9/2012	15.1	30.3	424	194	C	8:50
6/9/2012	22.0	46.3	313	387	A-C-A	11:40
6–7/9/2012	22.6	46.9	412	600	C-A-C	19:00
9–10/9/2012	9.1	21.5	195	98	A	7:50
10/9/2012	11.9	16.3	110	18	A	7:00
12–13/9/2012	7.9	12.4	102	33	Complicated	11:50
16/9/2012	12.5	20.7	247	104	Complicated	10:20
17–18/9/2012	14.8	34.3	178	179	C	13:20
25/9/2012	5.1	8.9	177	29	A	13:10
26/9/2012	14.8	46.7	529	405	Complicated	13:40
26–27/9/2012	23.7	47.4	664	518	A	10:20
27–28/9/2012	10.8	16.0	206	90	C	19:10

SSC, suspended sediment concentration; SSY, suspended sediment yield; A, anticlockwise; C, clockwise; ACA, anticlockwise-clockwise-anticlockwise; CAC, clockwise-anticlockwise-clockwise.

For the 23 events in the high rainfall months of June, July and August, the correlation coefficients are much smaller (Figure 8). The highest yields were not necessarily related to high peak flows. Some of the small events had the highest yields. This is likely related to the dependence of sediment yield on sediment availability from the agricultural areas and hillslopes during this time of the year. Although the number of October and November events is not representative enough to draw firm conclusions about the relationship between sediment yield and peak flows, the few events do suggest that peak flows are not directly correlated with sediment yield.

study in the highlands of Ethiopia (Vanmaercke *et al.*, 2010) suggested that the variations in SSC are mainly due

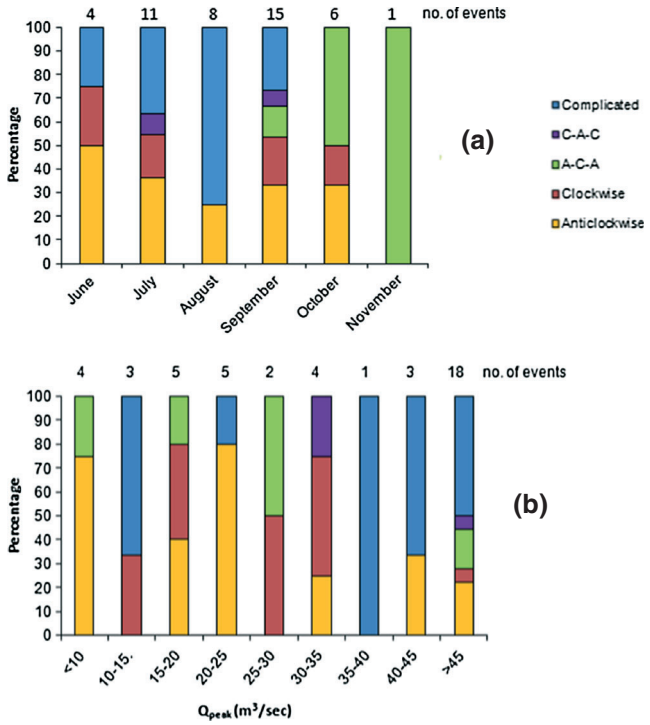

Figure 6. Percentage of hysteresis patterns observed for the considered 45 events (a) for each month and (b) versus peak discharge

to changes in sediment supply during the rainy season, which is related to the depletion of readily available sediments and the development of a vegetation cover. The modelling study of Easton *et al*. (2010) indicated that sediment delivery to the main stem of the Blue Nile is dominated by upland landscape erosion in the early part of the crop growing season when tillage occurs and before the soil is moistened and plant cover is established. They also suggested that once plant cover is established in mid-August, landscape erosion is negligible, and sediment export is dominated by channel processes. Similarly, White *et al*. (2010) indicated that erosion is controlled by channel factors rather than upland factors after mid-August when erosion controls switch from upland to channel factors. Figure 7 indeed indicates that sediment yield in our study area has a decreasing trend from mid-July till the end of September regardless of the magnitude of peak discharges. Zegeye *et al*. (2010) found the greatest rates of erosion early in the planting season, but they became negligible in August. In our study, the sediment yield significantly decreased from the end of August until the beginning of October while there were events with similar peak flows as those in June and July. This again suggests the depletion in dominant sediment sources, the ploughed crop fields, that led to a tremendous decrease in sediment yield in September, due to the effects of land cover. The decreasing trend of sediment yield after mid-August (Figure 7) for the same peak flows and the two distinct types of sediment patterns (Figure 8) also indicate that erosion rates for the main rainfall season significantly decrease after mid-August due to the effects of land use/cover. Figures 9 and 10 show the seasonal patterns of rainfall and vegetation cover [crop Normalized Difference Vegetation Index (NDVI)] of the West Gojam zone, which contains the study area of this paper. Crop NDVI, derived from satellite imagery, characterizes the general vegetation dynamics in the area (Verieling *et al*., 2011) and is used from crop monitoring. NDVI = 1 indicates the highest amount of green vegetation cover. Figures 9 and 10 clearly show the decrease in sediment yield with increasing crop vegetation cover while rainfall is still high.

Throughout the world, the relationship between SSC and water discharge (Q) during floods tends to be highly variable (Lenzi and Marchi, 2000). Some studies used the seasonal variability of SS data for generating sediment rating curves (Mossa, 1996), whereas other studies pointed out the need for a more detailed study at the time scale of individual flood events to improve the knowledge of sediment dynamics (Nadal-Romero *et al*.,

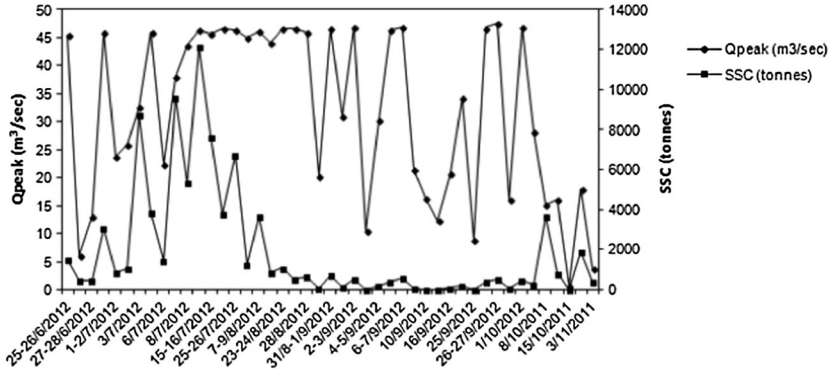

Figure 7. Suspended sediment concentration (SSC) and Q_{peak} of the considered events

2008). Vanmaercke *et al*. (2010) found very low correlations of the rating curves even after the data were stratified into three periods in a study conducted in a medium-sized catchment in the highlands of Ethiopia. Nadal-Romero *et al*. (2008) observed high sediment concentrations and a heterogeneous temporal distribution related to seasonal variations in surface run-off production for floods in a 0.45-km^2 humid Mediterranean bad land area in the Central Pyrenees. For our study area, based on the sediment yield of the 45 events and their corresponding peak discharges, Figure 8 shows two different sediment rating curves. The first relationship applies to events in August, September and the two October events; the second relationship applies to June, July, October and November. The first relationship shows better correlation ($R^2 = 0.82$) than the second one ($R^2 = 0.65$). The lower correlation coefficient of the second sediment rating curve is due to the high sediment yield associated with some of the low peak flows due to the abundant availability of loose sediment from the ploughed fields in this period of the year, as also observed from Figure 11 (a), (b) and (c). The rating curve for August, September and the first two October events is associated with lower sediment yields than the other curve for similar amounts of peak discharges, indicating there was a depletion of sediment from the sediment sources in September and August. These findings suggest that the agricultural fields (the pasture and crop fields) and hillslopes are more important sediment sources than the channels for most of the yearly rainy season.

Table II shows soil loss estimated by some studies conducted in Ethiopia. Regardless of the different figures, all the studies indicated the severity of soil erosion in the highlands of Ethiopia. On the basis of a 2010 land cover/use classification by Yeshaneh *et al*. (2013), the area upstream of the monitoring station of our study area that drains to the monitoring station consists of 5248 ha of cultivated land, 1848 ha of woody vegetation and 2742 ha

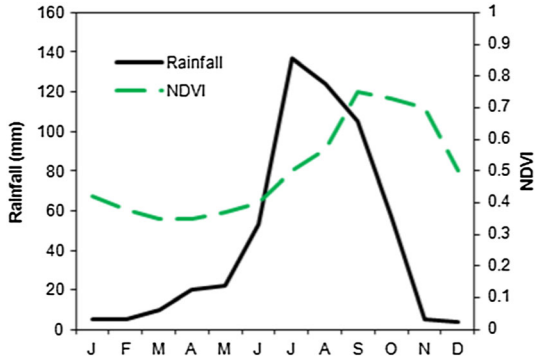

Figure 9. Average rainfall and crop Normalized Difference Vegetation Index for 1999–2006 for West Gojam zone (Province) of the Amhara region (EC-JRC, 2007)

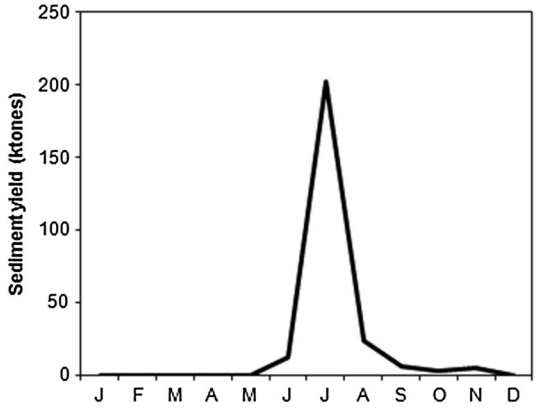

Figure 10. Sediment yield calculated for the study area (October 2011–September 2012)

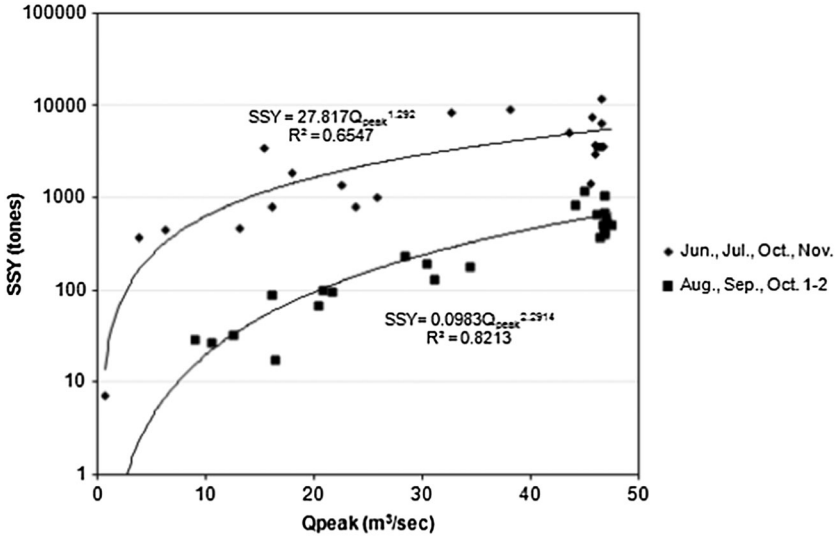

Figure 8. Sediment rating curves based on Q_{peak}

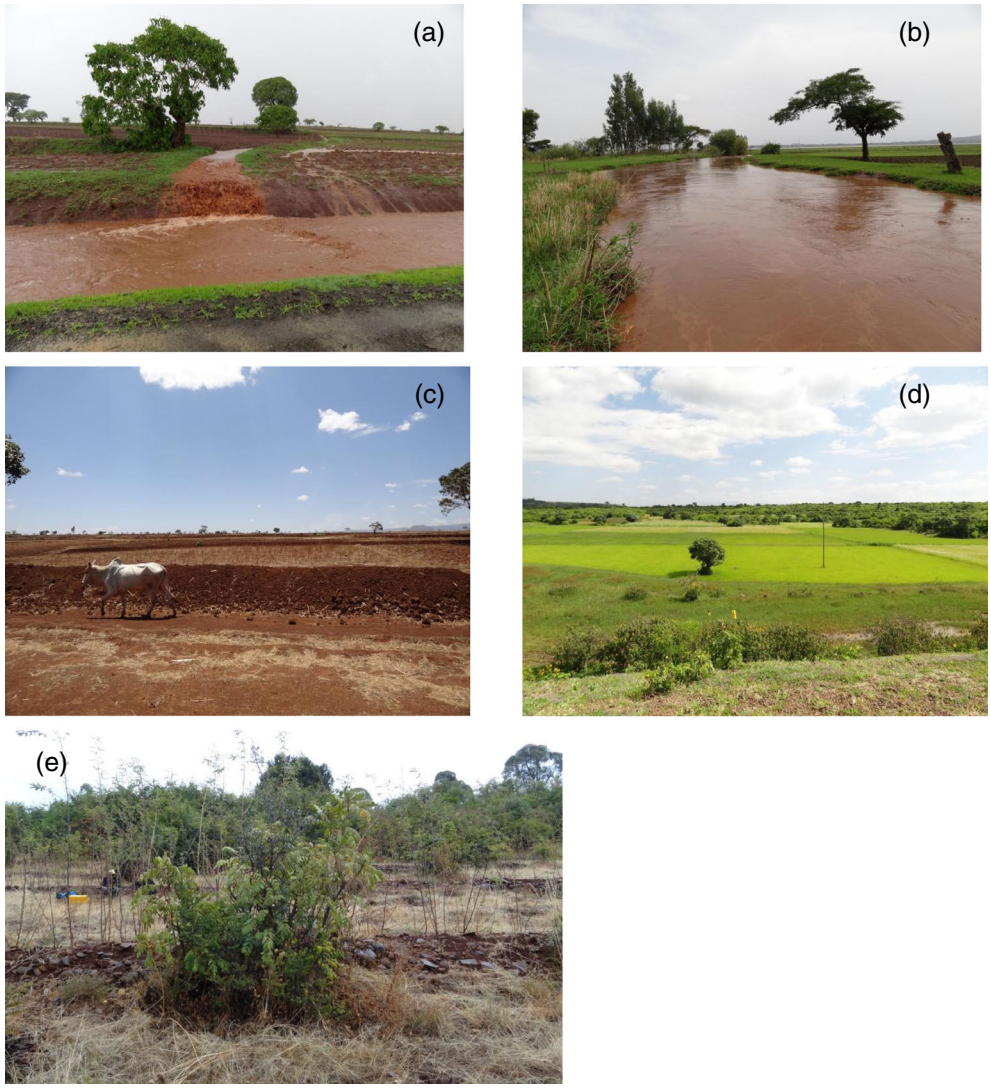

Figure 11. (a) June run-off from ploughed fields, (b) June flow at the monitoring station, (c) Land use/cover in June with soil conservation attempts (soil bunds), (d) Land use/cover in September and (e) soil and water conservation attempts (stone bunds with tree planting along with the stone bunds)

of other land use/cover types, that account for 53%, 19% and about 28% of the land use/cover of the area, respectively. Based on the fine temporal resolution (temporal resolution of 10 min) continuous discharge and sediment data we recorded at the monitoring station, we calculated a total sediment yield of 252 277 t year^{-1} from the 9838 ha, which is 25.6 t ha^{-1} year^{-1}. This figure is somewhat smaller than the findings of most of the studies conducted in the high lands of Ethiopia, although it is greater than sediment yields from catchments where effective soil and water conservation measures are practiced. This estimate is extremely high from an environmental point of view. The relatively low amount of sediment yield we estimated compared with previous studies could be attributed to various reasons. One possible reason could be our continuous measurement of discharge and sediment data with high temporal resolution, with better technology equipments than previous studies, which we believe has increased the reliability of sediment yield estimation, although there is a possibility of overestimation by previous studies with less regular monitoring. No studies have been performed in the catchment as to the extent the existing soil and water conservation structures have changed the sediment yield of the study area. Although there is a need for an in-depth study of the effect of the existing structures and other future additional options on soil erosion in the catchment, the existing structures might have contributed to reducing the sediment yield relative to estimates for the entire highlands of Ethiopia. It has been noted by Yeshaneh *et al.* (2013) that there is an increasing tendency to eucalyptus tree planting in the catchment in recent years; its impact on sediment yield should be studied along with the conservation measures.

Table II. Soil loss estimates by different studies in Ethiopia

	Study	Soil loss in $t\,ha^{-1}\,year^{-1}$	Estimated for	S and W conservation measures
1	Tadesse (2001)	31	Entire highlands	
2	Hurni (1993)	42	Plot based from cultivated fields in the highlands	
3	Nyssen *et al.* (2007)	14.8	199-ha agriculture-dominated catchment in the northern highlands of Ethiopia	Yes
4	Ethiopian highlands reclamation study (World Bank, 2007)	130	Plot based from cultivated lands	
5	Ethiopian highlands reclamation study (World Bank, 2007)	35	Entire highlands	
6	Vanmaercke *et al.* (2010)	4.97–65.43	513 300-ha (divided into subcatchments) agriculture-dominated catchment in Northern highlands	Yes
7	Guzman *et al.* (2013)	5.2, 24.7 and 7.4	477, 113 and 112-ha agriculture-dominated catchments in the highlands	Yes

Increased SS load due to intensive land use has been flagged out as a major concern by a number of studies in catchment and stream management (Restrepo *et al.*, 2006; Marttila and Klove, 2010). Schiettecatte *et al.* (2008) identified the highest soil losses from crop fields in a 151-km^2 subwatershed in Cuba at times when the soil is tilled and left bare for several weeks. They suggested that conservation measures would be most efficient during those times. If, in our study area, the erosion process continued at the same rate (assuming soil formation is negligible), the top 10 cm of soil will have been eroded in the next 50 years, which will leave the land extremely degraded, making agriculture not practicable at that time. Out of the total yearly sediment yield of 252 277 t, 91% is transported from early June to mid-August, which suggests that soil and water conservation measures need to particularly target this time of the year. This finding is in line with those of McHugh (2006), who indicated that severe erosion in a watershed in the highlands of Ethiopia is associated with a few erratic storms rather than steadily across all seasons. As stated by Food and Agriculture Organization, about 50% of the highlands of Ethiopia were already 'significantly eroded' in the mid-1980s, and erosion was causing a decline in land productivity at the rate of 2.2% per year (World Bank, 2007). The total area that drains to the reservoir, including the area downstream from our monitoring station, is 13 677 ha. With a sediment yield of 25.6 $t\,year^{-1}\,ha^{-1}$, it is also worth noting that a total volume of 269 000 m^3 of sediment reaches the Koga irrigation reservoir every year, which puts the sustainability of the irrigation dam in question.

CONCLUSIONS

We found anticlockwise hysteresis patterns between discharge and SSC to be dominant in the Koga catchment suggesting that the main sediment sources are the hillslopes and agricultural areas with smaller contributions from the river channels. However, there exist complex hysteresis types where the conclusions are less clear. During the period when the land is completely covered by vegetation, sediment yield associated with clockwise patterns was found to be greater than that associated with anticlockwise and other patterns, suggesting river channels contribute more to sediment yield in such conditions than the other sources. Complicated and other types of hysteresis patterns mostly associated with long events of multiple peaks suggest that a multitude of factors of sediment delivery in the study occur, which cannot be inferred from the hysteresis patterns. Sediment availability from the agricultural areas and hillslopes that depends on land use/cover was found to more strongly control the variations in event sedigraphs and rating loops than peak discharge. SSY–peak discharge plots indicated much lower sediment yield for the time after mid of August when the catchment was almost completely covered with vegetation as compared with similar events when the agricultural land was devoid of vegetation. Two distinct types of sediment rating curves based on peak discharges were observed for seasons with and without vegetation cover. SSY in the area is very high (25.6 $t\,ha^{-1}\,year^{-1}$), and 91% of the yearly SSY is transported from early June to mid-August because of the availability of loose sediment from the ploughed fields at this time of the year. If the erosion process continued at the

same rate, the top 10 cm of soil will have been eroded in the next 50 years. An amount of 269 000 m^3 of sediment reaches the Koga irrigation reservoir every year. This highlights the urgent need for appropriate soil and water conservation measures.

ACKNOWLEDGEMENTS

I would like to thank the Faculty for the Future Programme of the Schlumberger Foundation for granting me a scholarship to do my studies at the Vienna University of Technology. My thanks also extend to the Vienna Doctoral Programme on Water Resources Systems (DK-plus W1219-N22) for the technical and material support during my fieldwork in Ethiopia through the Austrian Science Funds and for hosting me in the programme. I would also like to thank the Koga Irrigation Project team, especially Ato Zerihun Balcha, for their cooperation towards the success of this project.

REFERENCES

Acers International Limited, and Shawel Consult International. 1995. Feasibility study of the Birr and Koga irrigation project. Koga Catchment & Irrigation Studies, Annex J.

Awulachew SB, Ahmed AA, Haileselassie A, Yilma AD, Bashar KE, McCartney M, Steenhuis T. 2010. Improved water and land management in the Ethiopian highlands and its impact on downstream stakeholders dependent on the Blue Nile. CGIAR Challenge Programme on Water and FOOD, CPWF Project Report, PN19, http://cgspace.cgiar.org/handle/10568/3908

Central Statistical Agency (CSA). 2007. *Population Census Data, Data Processing Department Data Archive*. Addis Ababa: Ethiopia.

Easton ZM, Fuka DR, White ED, Collick AS, Biruk Ashagre B, McCartney M, Awulachew SB, Ahmed AA, Steenhuis TS. 2010. A multi basin SWAT model analysis of runoff and sedimentation in the Blue Nile, Ethiopia. *Hydrology and Earth System Sciences* **14**: 1827–1841. DOI: 10.5194/hess-14-1827-2010.

EC-JRC. 2007. Crop monitoring in Ethiopia. Mars-Food, 03. hftp://mars.jrc.ec.europa.eu/bulletin/Ethiopia/2007/Bulletin_ETH_Sept07.pdf

Eder A, Strauss P, Krueger T, Quinton JN. 2010. Comparative calculation of suspended sediment loads with respect of hysteresis effects (in Petzenkirchen catchment, Austria). *Journal of Hydrology* **389**: 168–176.

Gao P, Josefson M. 2012. Event-based suspended sediment dynamics in a central New York watershed. *Geomorphology*: **139-140**: 425–437.

Gao P, Pasternack G, Bali K, Wallender W. 2007. Suspended-sediment transport in an intensively cultivated watershed in southeastern California, CATENA, **69**: 239–252.

Gao P, Pasternack G. 2007. Dynamics of suspended sediment transport at field-scale drain channels of irrigation-dominated watersheds in the Sonoran Desert, southeastern California. *Hydrological Processes* **21**: 2081–2092.

Gao P, Puckett J. 2011. A new approach for linking event-based upland sediment sources to downstream suspended sediment transport. *Earth Surface Processes and Landforms* **37**(2): 169–179.

Gentile F, Bisantino T, Corbino R, Milillo F, Romano G, Trisorio Liuzzi G. 2010. Monitoring and analysis of suspended sediment transport dynamics in the Carapelle torrent (Southern Italy). *Catena* **80**: 1–8.

Guzman CD, Tilahun SA, Zegeye AD, Steenhuis TS. 2013. Suspended sediment concentration-discharge relationships in the (sub-) humid Ethiopian highlands. *Hydrogy and Earth System Sciences* **17**: 1067–1077.

Hurni H. 1993. Land degradation, famine and resource scenarios in Ethiopia. In *World Soil Erosion and Conservation*, Pimentel D (ed). Cambridge University Press: Cambridge.

Jansson M. 2002. Determining sediment source areas in a tropical river basin, Costa Rica. *Catena* **47**: 63–84.

Lefrancois J, Grimaldi C, Gascuel-Odoux C, Gilliet N. 2007. Suspended sediment and discharge relationships to identify bank degradation as a main sediment source on small agricultural catchments. *Hydrological processes* **21**: 2923–2933.

Lenzi M, Marchi L. 2000. Suspended sediment load during floods in a small stream of Dolomites (northeastern Italy). *Catena* **39**: 267–282.

Lopez-Tarazon JA, Batalla RJ, Vericat D, Francke T. 2009. Suspended sediment transport in highly erodible catchment: the River Isabena (Southern Pyrenees). *Geomorphology* **109**: 210–221.

Marttila H, Klove B. 2010. Dynamics of erosion and suspended sediment transport from drained peatland forestry. *Journal of Hydrology* **388**: 414–425.

McHugh OV. 2006. Integrated water resources assessment and management in a drought-prone watershed in the Ethiopian Highlands. PhD dissertation presented to the Faculty of Graduate School of Cornell University, http://ecommons.library.cornell.edu/handle/1813/3384

Mossa J. 1996. Sediment dynamics in the lowermost Mississippi River. *Engineering Geology* **45**: 457–479.

Nadal-Romero E, Latron J, Marti-Bono C, Regües D. 2008. Temporal distribution of suspended sediment transport in humid Mediterranean badland area: the Araguas catchment, Central Pyrenees. *Geomorphology* **97**: 601–616.

Nyssen J, Poesen J, Moeyersons J, Haile M, Deckers J. 2007. Dynamics of soil erosion rates and controlling factors in the Northern Ethiopian Highlands – towards a sediment budget. *Earth Surface Processes and Landforms*. DOI:10.1002/esp.1569

Restrepo JD, Kjerfve B, Hermelin M, Restrepo JC. 2006. Factors controlling sediment yield in major South American drainage basin: the Magdalena River, Colombia. *Journal of Hydrology* **316**: 213–232.

Russel MA, Walling DE, Hodgkinson RA. 2001. Suspended sediment sources in two small lowland agricultural catchments in the UK. *Journal of Hydrology* **252**: 1–24.

Sadeghi SHR, Mizuyama T, Miyata S, Gomi T, Kosugi K, Fukushima T, Mizugaki S, Onda Y. 2008. Determinant factors of sediment graphs and rating loops in a reforested watershed, *Journal of Hydrology* **356**: 271–282.

Schiettecatte W, D'hondt L, Cornelis WM, Acosta ML, Leal Z, Lauwers N, Almoza Y, Alonso GR, Diaz J, Ruiz M, Gabriels D. 2008. Influence of land use on soil erosion risk in the Cuyaguateje watershed (Cuba). *CATENA* **74**: 1–12.

Shiferaw B, Holden S. 1999. Soil erosion and smallholders' conservation decisions in the highlands of Ethiopia. *World Development* **27**(4): 739–752.

Smith H, Dragovich D. 2009. Interpreting sediment delivery processes using suspended sediment-discharge hysteresis patterns from nested upland catchments, south-eastern Australia. *Hydrological processes* **23**: 2415–2426.

Tadesse G. 2001. Land Degradation: a challenge to Ethiopia. *Environmental Management* **27**(6): 815–826.

Tamene L, Vlek P. 2008. Soil erosion studies in northern Ethiopia, Chapter 5. Land use and soil resources, 73–100.

Vanmaercke M, Zenebe A, Poesen J, Neyssen J, Verstraeten G, Deckers J. 2010. Sediment dynamics and the role of flash floods in sediment export from medium-sized catchments: a case study from the semi-arid tropical highlands in northern Ethiopia. *Journal of Soils and Sediments* **10**: 661–627.

Verieling A, Beurs KM, Brown ME. 2011. Variability of African farming systems from phonological analysis of NDVI time series. *Climate Change* **109**: 455–477.

Walling DE, Webb BW. 1982. Sediment availability and the prediction of storm period sediment yields. In *Recent Developments in the Explanation and Prediction of Erosion and Sediment Yield*, Walling DE (ed). IAHS Press: Wallingford; 327–337 (IAHS Publications No. 137).

White ED, Easton ZM, Fuka DR, Collick AS, Adgo E, McCartney M, Awulachew SB, Selassie Y, Steenhuis TS. 2010. Development and application of a physically based landscape water balance in the SWAT model. *Hydrological Processes* **23**: 3728–3737. DOI:10.1002/hyp.7876.

World Bank. 2007. The cost of land degradation in Ethiopia: a review of past studies. © Washington, DC. https://openknowledge.worldbank.org/handle/10986/7939

Yeshaneh E, Wagner W, Exner-Kittridge M, Legesse D, Blöschl G. 2013. Identifying land use/cover dynamics in the Koga catchment, Ethiopia from multi-scale data, and implications for enviromnental change. *ISPRS International Journal of Geo-Information* **2**(2): 302–323.

Zegeye A, Steenhuis T, Blake R, Kidanu S, Collick A, Dadgari F. 2010. Assessment of soil erosion processes and farmer perception of land conservation in Debre Mewi watershed near Lake Tana, Ethiopia. *Ecohydrology & Hydrobiology* **10**(2-4): 297–306.

